Monoelectronic and dielectronic processes producing *K*-shell vacancies in slow $Ne^{q+}+CH_4$ collisions $(q=3-9)$

F. Frémont, C. Bedouet, X. Husson, and J.-Y. Chesnel
Centre Interdisciplinaire de Recherche Ions Lasers, Unité Mixte CEA-CNRS-ISMRA, Université de Caen Basse Normandie, 6 Bovlevard du Maréchal Juin, F-14050 Caen Cedex, France

N. Stolterfoht
Hahn-Meitner Institut, Bereich Festkörperphysik, Glienicker Strasse 100, D-14109 Berlin, Germany
(Received 7 May 1999)

Cross sections for Auger emission following the creation of a *K*-shell vacancy in C have been measured in slow collisions of Ne^{q+} with CH_4 $(q=3-9)$. Projectile energies ranging from 30 to 180 keV were investigated. For projectile charges lower than 7, the transfer of a *K* electron from C into the projectile is attributed to monoelectronic $2p\sigma$-$2p\pi$ transitions induced by rotational coupling at small internuclear distances. For higher charge states, the measured cross sections are found to be significantly larger at the lowest projectile energies than predicted cross sections for $2p\sigma$-$2p\pi$ transitions. It is shown that other mechanisms must be invoked, such as dielectronic excitation due to electron-electron interaction. Dielectronic excitation gives rise to a simultaneous transfer of inner- and outer-shell electrons of CH_4 into a 2ℓ shell of Ne.
[S1050-2947(99)06511-7]

PACS number(s): 32.80.Hd

I. INTRODUCTION

The mechanisms responsible for charge exchange in slow ion-atom collisions have received considerable attention during the last decades [1–7]. Much experimental and theoretical work has been devoted to collisions involving low-charged projectiles [1,8–12]. For such low-charged ion-atom collisions, the processes that contribute to the production of *K*-shell vacancies have been extensively studied [8–11]. Since the projectile velocity is smaller than that of the inner-shell electron involved, the creation of a vacancy in the *K* shell of a neutral target may be described using the molecular-orbital (MO) model [12,13]. Within this model, inner-shell vacancy transfer proceeds via coupling of the MO's formed during the collision. Figure 1 (left side) shows a schematic MO diagram for the system $Ne^{+}+C$. At large internuclear distances, the MO energies correlate to the orbital energies of C and Ne. At internuclear distances significantly smaller than the classical radii of the electronic orbitals of the collision partners, the MO energies correspond to the orbital energies of the equivalent united atom S. As illustrated in Fig. 1 for the collision system $Ne^{+}+C$, a two-step process is suggested to explain the production of $1s$ vacancy in C. First, at large internuclear distance, a vacancy may occupy the $2p\pi$ MO. As smaller internuclear distances are reached, the vacancy can be transferred from the $2p\pi$ MO to the $2p\sigma$ MO via a rotational coupling mechanism. It is noted that this mechanism is a one-electron process.

Cross sections for producing a target *K* vacancy via rotational coupling have been determined experimentally for many collision systems [1,14]. The cross sections were found to be nearly constant above a projectile energy threshold (~150 keV for $Ne^{+}+O$, for example). Below this energy limit, the cross sections rapidly decrease. These experimental results confirmed various theoretical calculations, which were performed to describe the rotational coupling between the $2p\pi$ MO and the $2p\sigma$ MO [15,16]. In general, good agreement between experimental results and theoretical predictions was shown for a large variety of symmetric and near-symmetric collision systems.

A detailed investigation of the projectile-charge dependence of *K*-shell vacancy production in slow collisions of light ions and atoms has been done by Fortner *et al.* [8]. For collision systems such as $Ne^{q+}+CH_4$ with low q values from 1 to 4, the measured total cross sections [8] were found to be enhanced when the projectile charge increases. It is noted that the experimental results (cf. Fig. 1 of Ref. [8]) were shown to be compatible with the static MO picture [17], in which the probability for *K*-shell vacancy production is assumed to be proportional to the number of $2p\pi$ vacancies initially present.

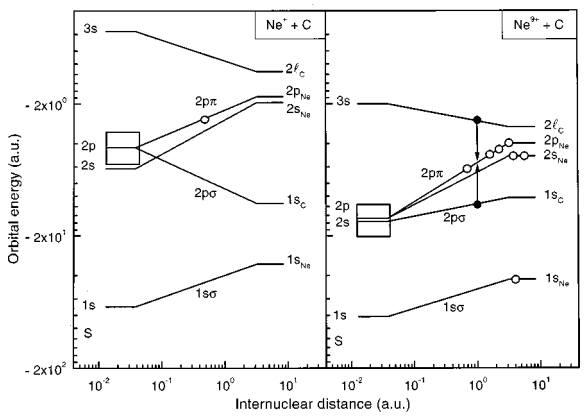

FIG. 1. Schematic MO energy diagrams for $Ne^{+}+C$ and $Ne^{9+}+C$ collisions. The squares indicate the regions where the rotational coupling takes place. For $Ne^{9+}+C$ collisions, resonance conditions for dielectronic excitation are visualized using vertical arrows.

Recently, the interaction of highly charged Ne^{9+} ions with an amorphous C surface was investigated at projectile energies as low as 250 eV, using low-resolution electron spectroscopy [18]. Besides projectile *K*- and *L*-Auger maxima, the spectra were observed to contain a structure at the electron energy of ~230 eV. This structure was interpreted to follow the creation of a *K*-shell vacancy in the C target. The corresponding cross sections for C *K*-Auger electron emission were found to be significantly larger than $10^{-18}\,cm^2$. Such large cross sections at very low impact energies are unexpected when the rotational coupling is assumed to be the unique mechanism responsible for the *K*-vacancy production.

Figure 1 (right side) describes schematic MO for the system $Ne^{9+}+C$. It is first seen that the main consequence of changing the charge of the projectile is that the MO curves are shifted to lower energies. Hence, at internuclear distances of ~1 a.u., in addition to rotational coupling (squares in Fig. 1), a one-step *two*-electron transfer may produce a vacancy in the *K* shell of C. Due to electron-electron interaction, a 2ℓ electron from C is deexcited, transferring its excess energy to the $1s$ target electron, which, in turn, is removed and promoted to the $2p\pi$ orbital of the transient molecule. This process, referred to as dielectronic excitation [19], provides a mechanism producing a vacancy in the *K* shell of the target in the case of highly charged systems.

Recently, experimental evidence for dielectronic excitation has been found in slow $N^{7+}+Ne$ collisions using the method of Auger electron spectroscopy [20,21]. It is noted that, for the $N^{7+}+Ne$ system, the target $1s$ orbital is much deeper than the projectile one. Hence, the rotational coupling is excluded for the target *K*-vacancy production [20,21]. On the contrary, for the system $Ne^{9+}+C$ (Fig. 1), the target $1s$ electron is less bound than the projectile $1s$ electron, allowing the rotational coupling to occur (see the squares in Fig. 1). Therefore, concerning the rotational and dielectronic processes, the question arises as to which process is favored in $Ne^{q+}+CH_4$ collisions when highly projectiles are used.

In this work, we studied C *K*-shell vacancy production in the collision system $Ne^{q+}+CH_4$. The choice of CH_4 instead of atomic C is justified by the fact that the presence of the four protons in CH_4 does not significantly affect the *K*-shell energy of carbon. After the removal of a *K*-shell electron from the carbon atom, the target is in an excited state, which may decay by means of the emission of Auger electrons. Hence, the $Ne^{q+}+CH_4$ collisions can be studied using target Auger spectroscopy. For projectile energies in the range 30–180 keV, projectile charges from 3 to 9 are investigated. Absolute cross sections for producing *K*-Auger electrons are extracted from Auger-electron measurements. From the comparison with previous experiments involving low-charged Ne^{q+} ions ($q \leq 4$), it is found that deviations from the expected cross sections due to rotational coupling occur for charges larger than 7. Such deviations indicate that the rotational coupling is not the only mechanism that is responsible for the production of *K*-shell vacancies in C.

II. EXPERIMENTAL METHOD

The measurements were carried out at the 14-GHz ECR ion sources at the Grand Accélérateur National d'Ions Lourds (GANIL) in Caen, using the electron-spectroscopy apparatus [22] from the Hahn-Meitner Institut (HMI), Berlin. Ions of Ne^{q+} ($q=3-9$) were extracted from the ECR source and collimated to a diameter of ~2 mm, with typical currents of about 10 nA. In the center of the scattering chamber, an effusive gas jet was installed to provide a beam of CH_4 molecules, which was used as the target. In the present experiment, care was taken to ensure single-collision conditions. The average target pressure was estimated to be $\sim 10^{-4}$ mbar. The fraction of charge states other than the primary one present in the incident beam was estimated to be ~15%.

Auger electrons emitted after the collision were energy analyzed using a single-stage spectrometer, which consists of an electrostatic parallel-plate analyzer [22]. To verify the angular dependence of the electron emission, the spectra were collected at several observation angles with respect to the beam direction. The intrinsic resolution of the analyzer was 5% full width at half maximum (FWHM). Since the spectrometer efficiency and the gas target pressure were determined from auxiliary measurements [23], absolute cross sections for Auger-electron emission could be obtained.

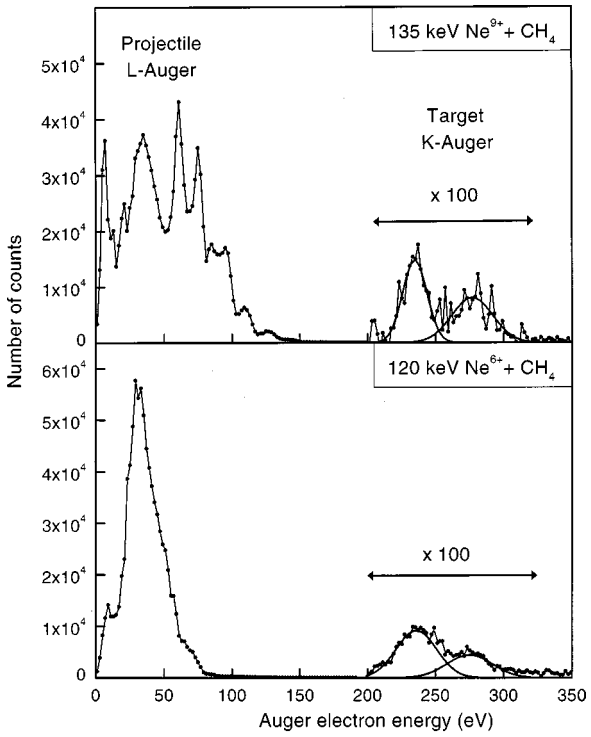

FIG. 2. Spectra of Auger electrons produced in 135-keV $Ne^{9+}+CH_4$ and 120-keV $Ne^{6+}+CH_4$ collisions at an observation angle of 150°. The peaks in the range 0–150 eV correspond to the decay of multiexcited states of the projectile. The groups of peaks centered at ~240 eV and ~275 eV originate from *K*-Auger emission of the C target.

III. ANALYSIS OF THE SPECTRA

Figure 2 shows typical Auger spectra for the systems $Ne^{6+}+CH_4$ and $Ne^{9+}+CH_4$ studied at impact energies of 120 and 135 keV, respectively. The spectra presented in the figure were recorded at an observation angle of 150° with respect to the incident-beam direction. It is noted that no

anisotropy for the Auger lines has been observed in the angular region from 80° to 160°. Two groups of Auger lines are clearly separated. In the electron energy range from 0 to 150 eV, the spectra show peaks attributed to electrons emitted by the projectile, whereas the group of lines in the range from 200 to 320 eV is attributed to the decay of the target. The origin of the Auger electrons from projectile and target was verified by analyzing the Doppler effect on the ejected Auger electrons. The Doppler effect due to the movement of the projectile leads to a shift of the peaks associated with the projectile when changing the observation angle. On the contrary, the group of peaks associated with the target is insensitive to the Doppler effect, because of the low velocity of the target after the collision.

The emission of the electrons in the range 0–150 eV follows the capture of two outer-shell electrons from the target into the configurations $3\ell n\ell'$ ($n \geq 3$). After the collision, these configurations decay to the $2\ell\varepsilon\ell'$ continuum by means of Auger transitions. Also, the capture of more than two outer-shell electrons leads to *L*-Auger emission. Moreover, *K*-Auger transitions following multiple-electron capture are observed in the electron-energy range from 550 to 850 eV.

Next, we examine the Auger peaks originating from the target. The emission of the electrons whose energy is in the range 200–260 eV is due to the capture of a *K*-shell electron from the C atom. In addition, a group of peaks centered at ~280 eV is observed. These peaks are due to the deexcitation of the target after the simultaneous capture of a *K*-shell electron from C and the excitation of a target outer-shell electron.

The single differential cross section $d\sigma_K^a/d\Omega$ for *K*-Auger electron emission associated with the capture of a *K*-shell electron from C was determined by integration of the spectra with respect to electron energy. The emission of Auger electrons was found to be isotropic within the experimental uncertainties. Thus, the total Auger electron emission cross section σ_K^a was derived by multiplying $d\sigma_K^a/d\Omega$ by 4π. The results are presented in Fig. 3 and Table I for the collision systems $Ne^{6+}+CH_4$ and $Ne^{9+}+CH_4$. Two different tendencies for the cross sections are clearly observed when the projectile charge varies from 6 to 9. First, we consider the system $Ne^{6+}+CH_4$. At the highest projectile energies, the total Auger electron emission cross section σ_K^a is of the order of $10^{-18}\,cm^2$. As the projectile energy decreases, it is seen that σ_K^a significantly decreases. For instance, at the lowest energy (i.e., 30 keV) the cross section σ_K^a is less than $10^{-19}\,cm^2$. On the contrary, for the system $Ne^{9+}+CH_4$, the cross section σ_K^a is found to remain constant as the projectile energy decreases down to 30 keV.

To proceed with the analysis of our experimental results, the present cross sections are compared with the previous data from Ref. [14]. In that work, collisions involving singly charged projectiles (B^+, C^+, N^+) and the CH_4 target were investigated in the same projectile-energy range as that presently studied (Fig. 4). The $Ne^+ + CH_4$ collision system was also analyzed. However, for the latter collision system only projectile energies in the range 200–500 keV (Fig. 4), i.e., significantly larger than the present energies, were explored [14]. For the $A^+ + CH_4$ collisions, total cross sections σ_{rot}^a for

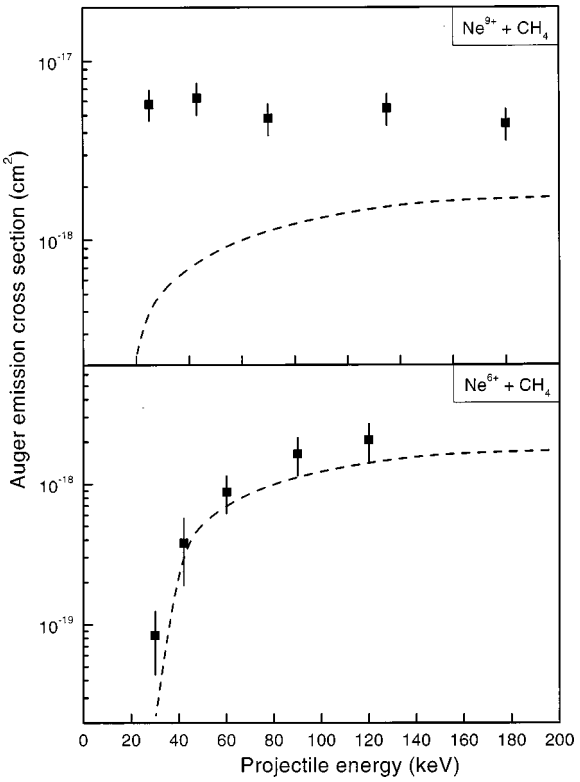

FIG. 3. Experimental cross sections (squares) associated with the production of a carbon-*K* vacancy in $Ne^{9+}+CH_4$ and $Ne^{6+}+CH_4$ collisions. Dashed curves represent the cross sections σ_{rot}^a for Auger-electron emission following the rotational coupling mechanism [Eq. (1)].

Auger-electron emission following the rotational coupling mechanism were measured [14]. From the results given in Table I of Ref. [14], the experimental cross sections σ_{rot}^a are found to be remarkably well fitted (dashed curves in Fig. 4) when using the empirical relation

$$\sigma_{rot}^a = N_1 a \ln(bE). \tag{1}$$

In this expression, the quantities *a* and *b* are fitting parameters and *E* is the energy of the projectile. The quantity N_1 is the probability that the $2p\pi$ orbital will contain one vacancy. It was shown previously that for asymmetric collision systems, N_1 is close to 1/3 [14]. For the projectiles with atomic number $Z=4$ to 7, *b* was found to be constant, while *a* depends on *Z* (Table II). Thus, the same value for *b* than that obtained for $Z=4$ to 7 was used to fit the experimental data for the collision system $Ne^+ + CH_4$ (solid line in Fig. 4). Hence, the quantity *a* could be determined for this system (Table II).

Since higher projectile charges are involved in the system $Ne^{q+} + CH_4$, the quantity N_1 must be replaced by N_q, which depends on the charge of the projectile [8], i.e., the number of vacancies present in the projectile prior to the collision. For charges $q=2-4$ the ratio $p_q = N_q/N_1$ was found to be equal to the charge *q* of the projectile [8]. This result is compatible with the static MO picture, in which the *K*-shell vacancy production is proportional to the number of $2p\pi$ vacancies initially present. However, for charges larger than

TABLE I. Auger emission cross sections $\sigma_K^a\,(10^{-19}\,\mathrm{cm}^2)$ after the creation of a K vacancy in C in $Ne^{q+}+CH_4$ collisions. The projectile charge q ranges from 3 to 9.

Projectile energy (keV)	Cross section $\sigma_K^a\,(10^{-19}\,\mathrm{cm}^2)$						
	$q=3$	$q=4$	$q=5$	$q=6$	$q=7$	$q=8$	$q=9$
25						9.2±1.8	
30	0.24±0.07	0.30±0.06		0.84±0.16			
35	1.0±0.4		1.6±0.3		4.2±0.8		
40		1.8±0.4		3.8±0.8		12.0±2.4	
45	2.5±0.8						57.5±11.5
50			4.5±0.9		5.8±1.2		
55						16.0±3.2	
60	3.6±1.2	5.8±1.2		8.8±1.8			62.3±12.4
70					17.6±3.6		
75			10.2±2.0				
80		8.5±1.7				24.8±5.0	
90				16.4±3.2			48.0±9.6
100			13.4±2.6		24.0±4.8		
120				20.6±4.2		36.8±7.4	
135							54.5±11.0
140					34.4±6.8		
160						37.0±7.4	
180							44.8±9.0

4, the quantity N_q is expected to be equal to 4, since the $2p\pi$ orbital contains only four vacancies.

For charges $q \leqslant 6$, the cross sections σ_{rot}^a derived from Eq. (1) using the above N_q values are found to agree well with our experimental results. For example, for $q=6$, the difference between σ_{rot}^a (dashed curves of Fig. 3) and our data do not exceed a factor of 1.5. Hence, it is likely that for charges up to $q=6$, the creation of a K-shell vacancy in C is governed by the mechanism of rotational coupling. For charges larger than 6, Eq. (1) can no longer fit our experimental results. As shown in Fig. 3 for the system $Ne^{9+}+CH_4$, our results are found to be significantly larger at low impact energies than the evaluated cross section σ_{rot}^a. To explain the deviations that occur for projectiles whose charges are larger than 6, calculations were performed within the framework of the molecular-orbital (MO) picture. Hence, contributions due to the rotational coupling process as well as to the dielectronic excitation process were evaluated.

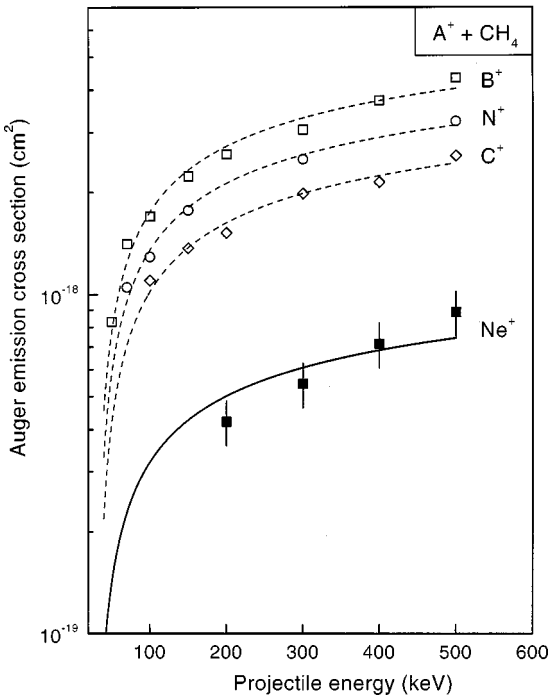

FIG. 4. Experimental cross sections associated with the production of a carbon-K vacancy in collisions of singly charged ions (B^+, C^+, N^+, and Ne^+) and CH_4 (from Ref. [14]). The uncertainties for the cross sections are about 15% [14]. Dashed curves are the result of the fitting procedure using relation (1). The solid line extrapolates experiment for $Ne^+ + CH_4$ collisions.

IV. CROSS SECTIONS FOR *K*-SHELL VACANCY PRODUCTION

A. Molecular orbitals and potential curves

The evaluation of the MO's has previously been described [24], so that a brief analysis is given here. The MO calcula-

TABLE II. Values of the fitting parameters a and b for Auger emission cross sections σ_{rot}^a [Eq. (1)] after the K-vacancy creation in C via a rotational coupling mechanism for B^+, C^+, N^+, and $Ne^+ + CH_4$ collisions (cf. Fig. 4). The experimental cross sections are taken from Ref. [14]. The uncertainties for a and b result from the standard deviation of the fitting procedure. In the case of $Ne^+ + CH_4$ collisions, an average value of 0.034 was taken for b.

Fitting parameters	B	C	N	Ne
$a\,(10^{-18})$	1.42±0.09	0.88±0.08	1.11±0.06	0.26±0.02
b	0.034±0.004	0.032±0.006	0.034±0.003	0.034

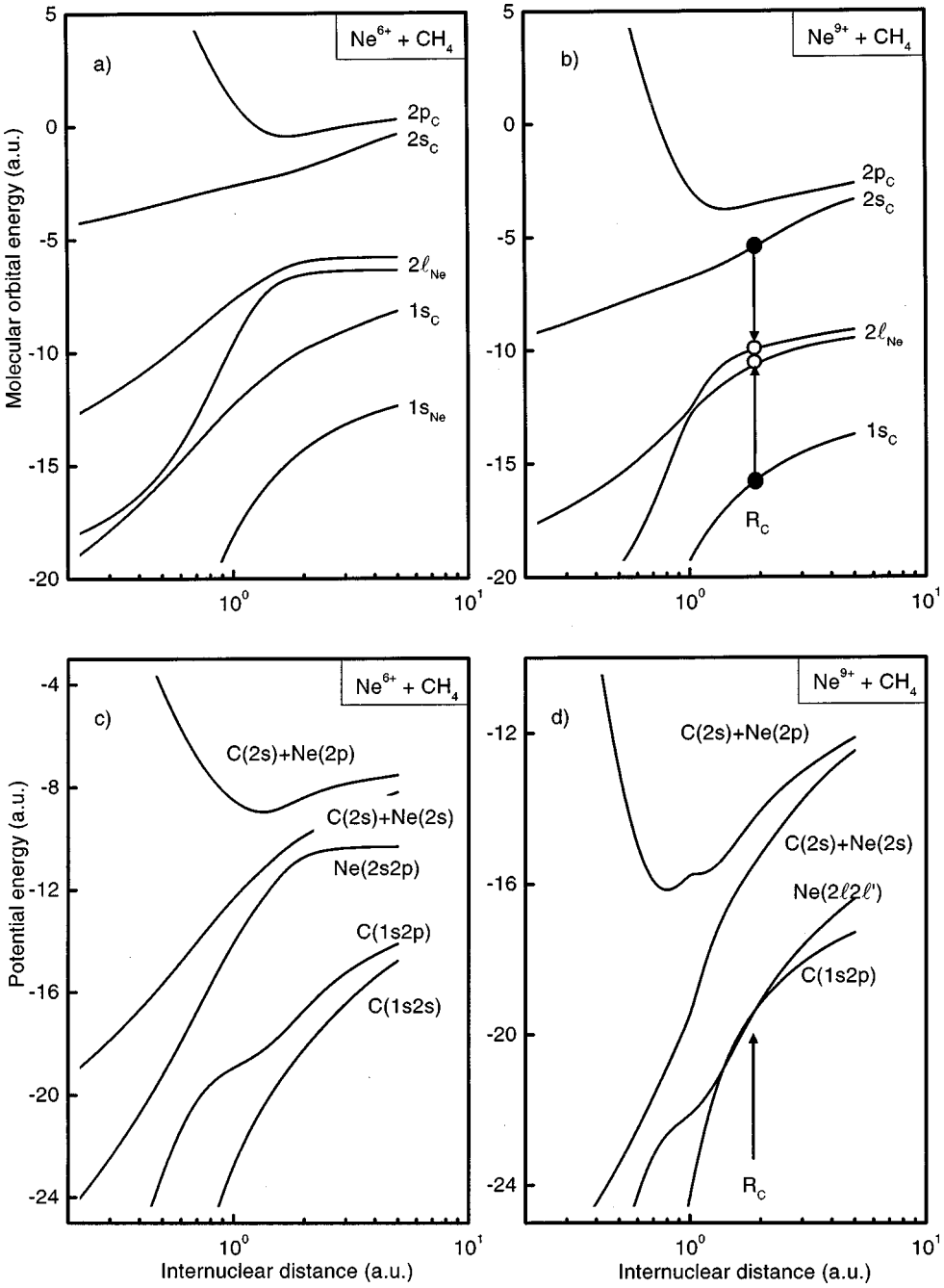

FIG. 5. MO curves (a), (b) and potential-energy curves (c), (d) for the collision systems $Ne^{6+}+CH_4$ and $Ne^{9+}+CH_4$ evaluated by diagonalization of model matrix elements [25]. The arrows represent the crossing at which the dielectronic excitation occurs. The quantity R_c refers to the internuclear distance at which the transition due to electron-electron interaction occurs.

tions are based on analytic matrix elements that have been evaluated within a screened hydrogenic model (SHM) [25]. The matrix elements depend on the binding energies of the electrons on each atomic center. The binding energies of $1s$ and 2ℓ orbitals of Ne were obtained, using the Hartree-Fock code by Cowan [26]. For the specific case of C in CH_4, the results by Vaeck and Zitane were used [27].

From the matrix elements, the corresponding MO energies were evaluated for each system $Ne^{q+}+CH_4 (q \geqslant 4)$ by means of numerical diagonalization. The results for σ orbitals are presented in Fig. 5, which refers to the systems $Ne^{6+}+CH_4$ and $Ne^{9+}+CH_4$ [Figs. 5(a) and 5(b), respectively]. At large internuclear distances, the MO energies correlate to the orbitals of C [28] and Ne. In the entrance channel, the electrons occupy the $1s$ and 2ℓ orbitals of C. In addition to the MO curves, the potential curves [Figs. 5(c) and 5(d)] obtained by addition of the MO curves of the associated active electrons were used for a quantitative determination of the internuclear distance R_c at which a transition may occur.

In the diagram that refers to the collision system $Ne^{6+}+CH_4$ no crossing appears [Fig. 5(c)] between the entrance channel [labeled $C(1s2p)$] and the $2\ell 2\ell'$ orbitals of Ne. Hence, a simultaneous two-electron transition due to electron-electron interaction is unlikely. Moreover, no crossing is visible between the entrance channel and the channels

$C(2\ell)+Ne(2\ell)$. Thus, a transfer of a *K*-shell electron from C into orbitals of Ne is also unlikely to occur by means of radial coupling. Therefore, the unique process that is responsible for a *K*-shell vacancy in C is the rotational coupling mechanism, which occurs at internuclear distances of the order of 0.01 a.u. (not shown in Fig. 5). At small internuclear distances, a shift in energy induced by the increase of the projectile charge is seen in the system $Ne^{9+}+CH_4$ [Fig. 5(b)], as mentioned in the Introduction. Consequently, resonance conditions are created for a dielectronic excitation process leading to a *K* vacancy in the C atom [arrows in Figs. 5(b) and 5(d)], where an electron from a high-lying level is deexcited, transferring its excess energy to a $1s$ electron, which, in turn, is transferred into the 2ℓ orbital of Ne.

B. Cross sections

For $Ne^{9+}+CH_4$ collisions, the potential energies [Fig. 5(d)] were used to calculate probabilities for the transfer of two $1s$ and 2ℓ electrons from C into the *L* shell of the Ne projectile. Depending on the mechanisms involved, two models were used in the analysis. First, cross sections $\sigma_{\rm diel}$ for producing a *K* vacancy in the C atom by means of the dielectronic excitation process were determined applying the Landau-Zener model [29] at curve crossings with internuclear distances R_c. Second, the theoretical *K*-excitation probabilities by Taulbjerg *et al.* [16] were utilized to describe the rotational coupling mechanism and to evaluate the corresponding cross sections $\sigma_{\rm rot}$.

At an internuclear distance R_c the probability $p_{\rm diel}$ for a transition between initial state (1) and final state (2) due to dielectronic excitation, is given by

$$p_{\rm diel}(b)\approx\exp\left(-\frac{2\pi|H_{12}|^2}{v_R(b)\Delta F(R_c)}\right), \tag{2}$$

where b is the impact parameter, $v_R(b)$ is the radial velocity, and $\Delta F(R_c)$ is the measure for the relative inclination of the potential curves at the crossing radius R_c. The nondiagonal matrix element $H_{12}(R_c)$ describes the dielectronic interaction at R_c. It is noted that only little is known about this quantity. However, previous evaluations have shown that a value of the order of 0.05 a.u. for $H_{12}(R_c)$ is quite reasonable [19,21]. Hence, this value was retained in the present calculations.

To account for the rotational coupling mechanism, an analytic expression of the probability $p_{\rm rot}(b)$ for *K*-shell excitation was derived from calculations (cf. Fig. 3 of Ref. [16]). With good accuracy, $p_{\rm rot}(b)$ is given by

$$p_{\rm rot}(b)=A(v)b^2\exp(-\alpha b^2), \tag{3}$$

where $A(v)$ and α are fitting parameters. In the case of $Ne^{9+}+CH_4$ collisions, the quantity α was found to be constant ($\sim$454) in the energy range explored, while A depends on the projectile velocity v. The quantity $A(v)$ was determined using the cross sections deduced from Eq. (1) for the system $Ne^{+}+CH_4$.

The total probabilities $P_{\rm rot}$ and $P_{\rm diel}$ for the transfer of an inner-shell electron from C are

$$P_{\rm rot}=(1-p_{\rm diel})p_{\rm rot}(1-p_{\rm rot}), \tag{4a}$$

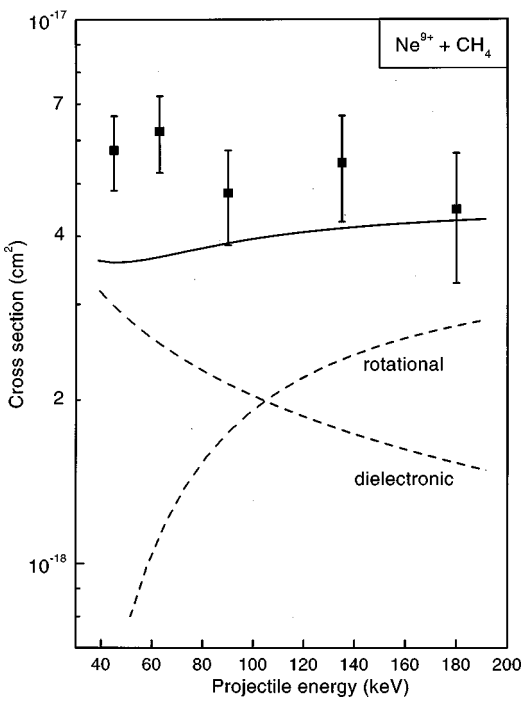

FIG. 6. Experimental cross sections (squares) and calculated total cross sections (full curves) associated with the production of a carbon-*K* vacancy in $Ne^{9+}+CH_4$. The contributions $\sigma_{\rm rot}$ and $\sigma_{\rm diel}$ (dashed curves) due to the rotational coupling mechanism and dielectronic excitation, respectively, are obtained from model calculations described in Sec. IV.

$$P_{\rm diel}=p_{\rm diel}(1-p_{\rm diel})(2-p_{\rm rot}), \tag{4b}$$

where the labels (rot) and (diel) refer to the rotational mechanism and the dielectronic excitation, respectively.

Finally the cross sections $\sigma_{\rm rot}$ and $\sigma_{\rm diel}$ are given by

$$\sigma_{\rm rot}=\int_0^{R_c}2\pi bP_{\rm rot}(b)db, \tag{5a}$$

$$\sigma_{\rm diel}=\int_0^{R_c}2\pi bP_{\rm diel}(b)db. \tag{5b}$$

The results of the calculations are reported in Fig. 6 for the collision system $Ne^{9+}+CH_4$ as a function of the projectile energy. First, it is seen that the total calculated cross sections (full line) are in rather good agreement with our experimental values since they are found to be nearly constant in the projectile energy range investigated here. The differences between calculation and experiment do not exceed a factor of 2. At the highest energies, the major contribution is found to originate from the rotational coupling mechanism. Nevertheless, it has to be noted that the relative contribution $\sigma_{\rm diel}$ of dielectronic excitation is not negligible, since it represents $\sim$30% of the total cross section. As the projectile energy decreases, the contribution of $\sigma_{\rm diel}$ increases and becomes dominant below projectile energies of about 80 keV. Hence, dielectronic excitation plays an essential role when high projectile charges are involved. This finding is consistent with our previous results [21], showing that

the dielectronic excitation process is responsible for the creation of a *K*-shell vacancy in Ne when bare N^{7+} ions are used.

V. CONCLUSION

In the present work, mechanisms responsible for the creation of a *K* vacancy in C following collisions between Ne^{q+} ions ($q=3-9$) and the CH_4 target are studied. Projectile energies ranging from 30 to 200 keV are investigated. For projectile charges up to $q=6$, the strong velocity dependence of the Auger emission cross section and a comparison with previous experiments [21] clearly show that the rotational coupling is the essential mechanism that is responsible for the production of a *K*-shell vacancy in C.

For higher projectile charges, it is found that the cross sections noticeably deviate from the expected cross section assuming only the rotational coupling mechanism. For the extreme case of $q=9$, the experimental cross sections are found to be nearly constant in the whole range of projectile energies studied. The mechanisms for the creation of a *K* vacancy in the target are discussed under the perspective of dynamic electron-electron interaction. The discussion is based on molecular-orbital diagrams that show that for charges larger than 6 resonance conditions are created for the transfer of two active electrons via the process of dielectronic excitation.

Applying the Landau-Zener model [29] for the specific case $q=9$, it is first seen that calculated total cross sections are in good agreement with experiment. The rotational coupling mechanism is found to be dominant at projectile energies larger than 120 keV. On the contrary, as the projectile energy decreases, the contribution of the dielectronic excitation process is found to increase. Hence, the present work provides clear evidence that when highly charged ions are involved, the role of the dielectronic excitation process is substantial for the production of inner-shell vacancies in atoms.

ACKNOWLEDGMENTS

We thank D. Lecler, J.-Y. Paquet, R. Leroy, and A. Lepoutre for their generous assistance during the experiments. This study was supported by the Program d'Actions Intégrées Franco-Allemand PROCOPE under Contract No. 98089.

[1] D. Schneider and N. Stolterfoht, Phys. Rev. A **24**, 2438 (1981).
[2] N. Stolterfoht, C. C. Havener, R. A. Phaneuf, J. K. Swenson, S. M. Shafroth, and F. W. Meyer, Phys. Rev. Lett. **57**, 74 (1986).
[3] L. R. Andersson, J. O. Pedersen, A. Barany, J. P. Bangsgaard, and P. Hvelplund, J. Phys. B **22**, 1603 (1989).
[4] F. Frémont, K. Sommer, D. Lecler, S. Hicham, P. Boduch, X. Husson, and N. Stolterfoht, Phys. Rev. A **46**, 222 (1992).
[5] A. Bordenave-Montesquieu, P. Benoît-Cattin, A. Gleizes, A. I. Marakchi, S. Dousson, and D. Hitz, J. Phys. B **17**, L127 (1984).
[6] C. Harel, H. Jouin, and B. Pons, J. Phys. B **24**, L425 (1991).
[7] H. Van der Hart, N. Vaeck, and J. E. Hansen, J. Phys. B **28**, 5207 (1995).
[8] R. J. Fortner, P. H. Woerlee, S. Doorn, Th. P. Hoogkamer, and F. W. Saris, Phys. Rev. Lett. **39**, 1322 (1977).
[9] C. L. Cocke, R. R. Randall, S. L. Varghese, and B. Curnutte, Phys. Rev. A **14**, 2026 (1976).
[10] N. Luz, S. Sackmann, and H. O. Lutz, J. Phys. B **12**, 1973 (1979).
[11] R. Shanker, U. Wille, R. Bilau, R. Hippler, W. R. McMurray, and H. O. Lutz, J. Phys. B **17**, 1353 (1984).
[12] U. Wille and R. Hippler, Phys. Rep. **132**, 129 (1987).
[13] J. Eichler, U. Wille, B. Fastrup, and K. Taulbjerg, Phys. Rev. A **14**, 707 (1976).
[14] D. Schneider and N. Stolterfoht, Phys. Rev. A **19**, 55 (1979).
[15] J. S. Briggs and J. H. Macek, J. Phys. B **6**, 982 (1973).
[16] K. Taulbjerg, J. S. Briggs, and J. Vaaben, J. Phys. B **9**, 1351 (1976).
[17] J. S. Briggs and J. H. Macek, J. Phys. B **6**, 841 (1973).
[18] M. Grether, D. Nieman, and N. Stolterfoht (private communication).
[19] N. Stolterfoht, Phys. Scr. **46**, 22 (1993).
[20] F. Frémont, C. Bedouet, J.-Y. Chesnel, H. Merabet, X. Husson, M. Grether, A. Spieler, and N. Stolterfoht, Phys. Rev. A **54**, R4609 (1996).
[21] C. Bedouet, F. Frémont, J.-Y. Chesnel, X. Husson, H. Merabet, N. Vaeck, N. Zitane, B. Sulik, M. Grether, and A. Spieler, Phys. Rev. A **59**, 4399 (1999).
[22] N. Stolterfoht, Z. Phys. **248**, 81 (1971); **248**, 92 (1971).
[23] N. Stolterfoht, K. Sommer, J. K. Swenson, C. C. Havener, and F. W. Meyer, Phys. Rev. A **42**, 5396 (1990).
[24] N. Stolterfoht, Phys. Rep. **146**, 315 (1987).
[25] N. Stolterfoht, in *Progress in Atomic Spectroscopy*, edited by H. Kleinoppen (Plenum, New York, 1987), Pt. D, p. 415.
[26] R. D. Cowan, *The Theory of Atomic Structure and Spectra* (University of California Press, Berkeley, 1981).
[27] N. Vaeck and N. Zitane (private communication).
[28] In the present discussion, the CH_4 molecule is considered as a simple atom with two electrons in the *K* shell and eight electrons in an *L* shell.
[29] C. D. Landau, J. Phys. (Moscow) **2**, 46 (1932); C. Zener, Proc. R. Soc. London, Ser. A **137**, 696 (1932).